Advances in Geo-Energy Research

Vol. 11, No. 3, p. 208-219, 2024

Original article

Rock permeability evolution during cyclic loading and colloid migration after saturation and drying

Evgenii Kozhevnikov[1]*, Mikhail Turbakov[1], Evgenii Riabokon[1], Evgenii Gladkikh[1], Mikhail Guzev[2], Arina Panteleeva[1], Zakhar Ivanov[1]

[1]*Department of Oil and Gas Technologies, Perm National Research Polytechnic University, Perm 614000, Russia*

[2]*Institute of Applied Mathematics, Far Eastern Branch of the Russian Academy of Sciences, Vladivostok 690000, Russia*

Keywords:
Permeability
coreflooding
colloid's migration
porous material
cyclic loading
Rehbinder effect

Cited as:
Kozhevnikov, E., Turbakov, M., Riabokon, E., Gladkikh, E., Guzev, M., Panteleeva, A., Ivanov, Z. Rock permeability evolution during cyclic loading and colloid migration after saturation and drying. Advances in Geo-Energy Research, 2024, 11(3): 208-219. https://doi.org/10.46690/ager.2024.03.05

Abstract:
The study of the influence of cyclic loading on the permeability of rocks has been conducted for a long time. Despite the extensive research database, the actual reasons for the decrease in permeability during loading have not been fully revealed. One of these reasons, as described in the research, is the migration of colloids. This paper presents the findings of a study on colloid migration as one of the causes of permeability degradation in porous rocks under cyclic loading. Permeability is measured by injecting nitrogen at a constant pressure. The cyclic loading program is designed to eliminate the effects of residual deformations, creep, and gas slippage. Direct and reverse nitrogen blowings with increased injection pressure were performed between loading cycles. These blowings promote colloidal movement within the porous medium, blocking pore throats and changes in permeability. A notable aspect of this work is that cyclic testing was performed before and after the saturation and drying procedure. Stuck colloids that cannot be moved by blowing are mobilized during saturation and drying. Comparative tests of cores after saturation and drying confirm the effect of colloid migration on permeability and enable the examination of whether plastic deformations caused permeability degradation in previous loading cycles. Additionally, it was observed that when saturated, new colloids can detach due to the Rehbinder effect, significantly reducing permeability.

1. Introduction

Currently, using porous underground rocks as natural reservoirs for storing natural gas and hydrogen is highly relevant (Liu et al., 2010; Metwally and Sondergeld, 2011; Heller et al., 2014; Wu et al., 2023). Aquifers and depleted oil and gas fields are used for underground gas storage (Siqueira et al., 2014; Haghi et al., 2018; Gao et al., 2020; Ge et al., 2022; Almutairi et al., 2023). During the operation of natural reservoirs, the injection and extraction of gases cause seasonal cyclic changes in reservoir pressure. These cyclic pressure fluctuations gradually degrade the reservoir properties, resulting in decreased efficiency and reduced service life of the reservoirs (Yang et al., 2015; Vogler et al., 2016; Anyim and Gan, 2020; Zhou et al., 2020; Kluge et al., 2021). To predict the performance characteristics of reservoirs, it is necessary to model the changes in permeability during cyclic filling and emptying. To achieve this, rock samples are tested under laboratory conditions using cyclic confining pressure to simulate variations in pore pressure (Yang and Hu, 2018; Lei et al., 2020; Liu et al., 2020; Xin et al., 2021; Wang et al., 2022; Kozhevnikov et al., 2023). Numerous experimental studies have observed that the curves depicting the reduction and restoration of permeability under loading are most accurately represented by power law functions (Li et al., 2014; Zheng et al., 2015; Milsch et al., 2016; Kozhevnikov et al., 2021; Nolte et al., 2021; Stanton-Yonge et al., 2023). Experimental equations may be the most straightforward approach to model permeability. However, when cyclic loading is involved, the permeability of rocks tends to decrease gradually. Further-

Yandy Scientific Press

*Corresponding author.
E-mail address: kozhevnikov_evg@mail.ru (E. Kozhevnikov); msturbakov@gmail.com (M. Turbakov); riabokon@pstu.ru (E. Riabokon); gladkih.ea@mail.ru (E. Gladkikh); guzev@iam.dvo.ru (M. Guzev).

Received December 4, 2023; revised January 10, 2024; accepted January 29, 2024; available online February 6, 2024.

more, the permeability curves do not align across all cycles, and permeability hysteresis becomes apparent (Selvadurai and Głowacki, 2008; Civan, 2021).

Typically, authors attribute the decrease in permeability for porous and fractured rocks under cyclic loading primarily to mechanical compaction (Hofmann et al., 2016; Yang and Hu, 2018; Blöcher et al., 2019; Chen et al., 2022; Wang et al., 2022). Elastic and plastic deformations during loading result in a reduction of pore channel size and a decrease in hydraulic conductivity. During unloading, the flexible expansion of pore channels partially restores permeability, but not entirely. To accurately assess the impact of mechanical compaction on permeability, it is essential to determine the extent to which elastic and plastic deformations contribute to the decrease in permeability. It is also necessary to examine whether plastic deformations permeability at relatively low loads, considering the Kaiser effect, which suggests the absence of irreversible deformations.

2. Materials and methods

Eight dry samples were used in this study – four porous limestone samples and four sandstone samples (with a diameter of 30 mm and length of 30 mm) obtained from a depth of 1,500 m. These rocks were oil-bearing and were sourced from the C1bb and C2b formations in the Perm region of Russia. The properties of the rock samples are presented in Table 1.

Evaluating the impact of mechanical compaction on permeability poses a challenge because current methods measure apparent permeability, not true permeability. The movement and transportation of colloids in a porous medium occur during the flow of fluids and gases (Bedrikovetsky et al., 2011; Torkzaban et al., 2015; Deb and Chakma, 2022; Kozhevnikov et al., 2022b; Wang et al., 2023). However, routine core tests do not assess the effect of colloids on permeability (Raziperchikolaee, 2023). Previous studies (Kozhevnikov et al., 2022a, 2023) have shown that the measured permeability can be influenced by colloidal migration during fluid and gas injection. While a decrease in permeability was observed in samples upon kerosene injection (Kozhevnikov et al., 2022b), the effect of colloid migration on rock transport properties was not always observed during nitrogen injection (Kozhevnikov et al., 2023). Due to their low viscosity and detachment forces, the low mobilization activity of gases necessitates high-gradient blowings between loading cycles to assess the presence of colloids in core samples and their impact on permeability. Blowings between loading cycles can lead to a 20% decrease in permeability through colloid migration, but experimental studies have shown that blowings did not change permeability in all samples. At the end of testing, an equilibrium state was established in the samples, in which colloid migration was no longer possible, and some pores were blocked, resulting in unchanged permeability. This raises questions: Were no colloids present in the samples with constant permeability, or were they not formed during cyclic loading? After testing in samples with stable permeability, is further colloid migration possible, and would it cause an increase or decrease in permeability? Can the samples be cleaned from colloids, and what would be the resultant permeability?

These questions can be answered by directly observing the pore space, such as computed tomography (CT). Computed tomography allows for the evaluation of the internal structure of rocks and any changes that may occur. Assessing the structure of rocks is a relatively simple task, even at low resolution. However, identifying subtle changes becomes challenging, even with high resolution and under significant loads, as in the example of work (Hu et al., 2020), where the confining pressure reaches 36 MPa, and changes in the structure are barely noticeable. It is important to note that the accuracy of comparative tomography is influenced by the presence of reference points and the precision of sample positioning during tomography. Even a slight displacement of tomogram layers during scanning significantly affects the final image and complicates the identification of changes in the porous medium after loading. In situ measurements can address this issue but require specialized equipment that may not always be available in core research institutes. Therefore, there is a need for simple and accessible testing methods to assess the effect of colloids on the permeability of rock samples. To evaluate the factors contributing to the final change in permeability, we have proposed a new technique, outlined below.

The structure of the samples was studied using scanning electron microscopy and CT. Based on the tomography results, three-dimensional (3D) models (Fig. 1(a)) and the connected pore space of the samples were obtained (Fig. 1(b)). Tomography showed the relative homogeneity of the samples and the absence of cracks and compactions, which allows for comparative studies and acceptance of these samples as homogeneous. The resulting microphotographs clearly show the mineral grains (quartz crystals in Fig. 1(c)), pores, and tiny particles with sizes of several microns, fragments of mineral grains and cement. Grains, small pores, and colloids (Fig. 1(c)) and their sizes are not distinguishable on CT scans with a resolution of 30 μm (Fig. 1(b)), which is a common problem when using microtomographs. However, even the use of nanotomography does not allow for assessing the movement of colloids inside the pores. This is because colloids are usually attached to the pore walls, making them difficult to distinguish from the rock matrix. Additionally, tomography determines the integral porosity, and the contribution of colloids to porosity is minimal, with their movement within neighboring pores hardly noticeable. Our CT studies (Kozhevnikov et al., 2023) showed no changes in the porous medium after cyclic testing. However, the permeability of some samples decreased significantly at the end of testing. To investigate the factors influencing the final decrease in permeability, a new approach was proposed by saturating and drying the samples between cyclic testing. The research methodology is shown below:

Primary testing

1) Preparation of core samples. Preparation was carried out according to standard methods, and samples were cleaned and dried to constant weight;
2) Samples are installed in a core holder of UltraPoroPerm-500;
3) In the core holder, an initial confining pressure of 2.76

Table 1. Rock samples used in the research and their properties.

No.	Rock type	Porosity, %	Initial permeability, 10^3 μm^2		Mass, g		Grad$P$, MPa/m
			Before S/D	After S/D	Before S/D	After S/D	
1	Limestone	14.79	35	46	47.589	47.587	0.621
6	Limestone	14.14	346	370	46.684	46.684	0.046
9	Limestone	14.97	156.1	146	46.174	46.173	0.131
20	Limestone	15.63	40.8	34	45.446	45.447	0.518
51	Sandstone	11.58	13.1	9.28	37.484	37.464	0.502
61	Sandstone	11.08	6.96	6.37	41.880	41.844	0.883
131	Sandstone	15.19	134.1	140.7	38.777	38.753	0.047
181	Sandstone	15.19	442.5	463.3	41.469	41.427	0.014

Notes: S/D-saturation drying procedure.

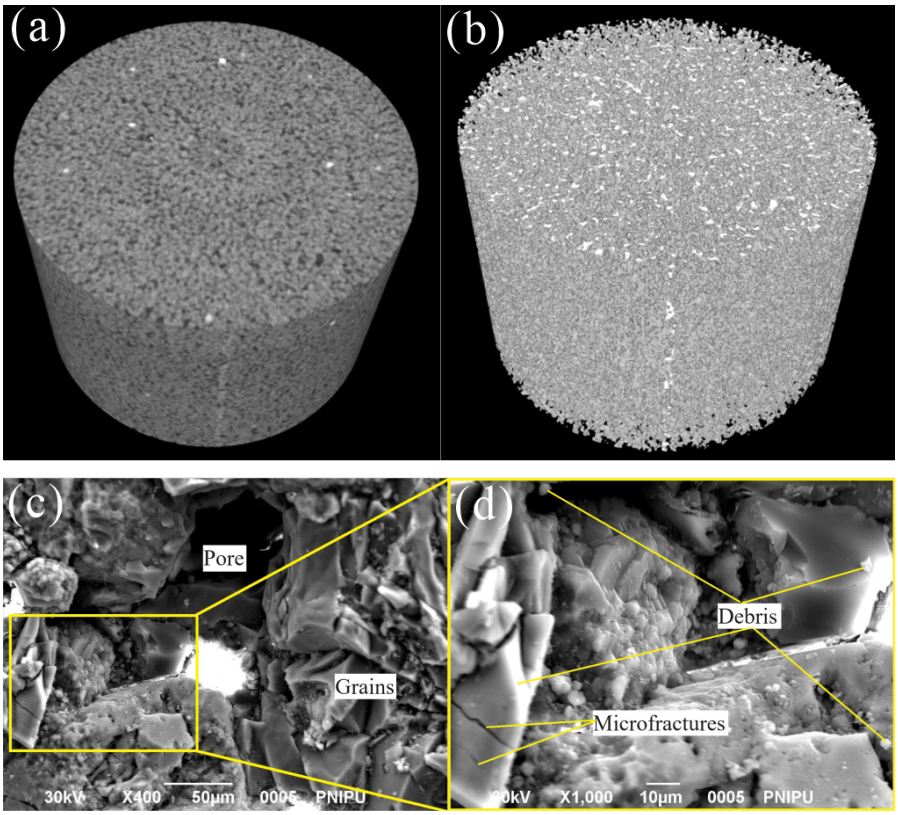

Fig. 1. (a) 3D model of a sandstone sample obtained using CT results (Diameter: 30 mm), (b) connected pore space of a sandstone sample, with voids shown in black and matrix in shades of gray, (c) magnification ×400 and (d) magnification ×1000 of the surface of Sample 51, and (d) micrograph ×1000 of the surface of Sample 51.

MPa is created, the sample is held for 30 minutes;

4) The first cycle of core testing while injecting nitrogen constantly. Nitrogen was injected constantly throughout the study to minimize the slippage effect. During injection, confining pressure changed according to the program (Fig. 2). Initial confining pressure-2.76 MPa, maximum-13.8 MPa, pressure step-2.76 MPa, injection time at each step-2∼3 minutes. During tests, sensor data was recorded on a computer one measurement per second. Based on the data obtained, instantaneous permeability (k) is calculated using the Darcy equation:

$$k = \frac{2\mu QLP_a}{S(P_{in}^2 - P_a^2)} \quad (1)$$

where μ is the viscosity of nitrogen (Pa·s), Q is the flowrate (m^3/s), L is the length of the sample (m), P_a

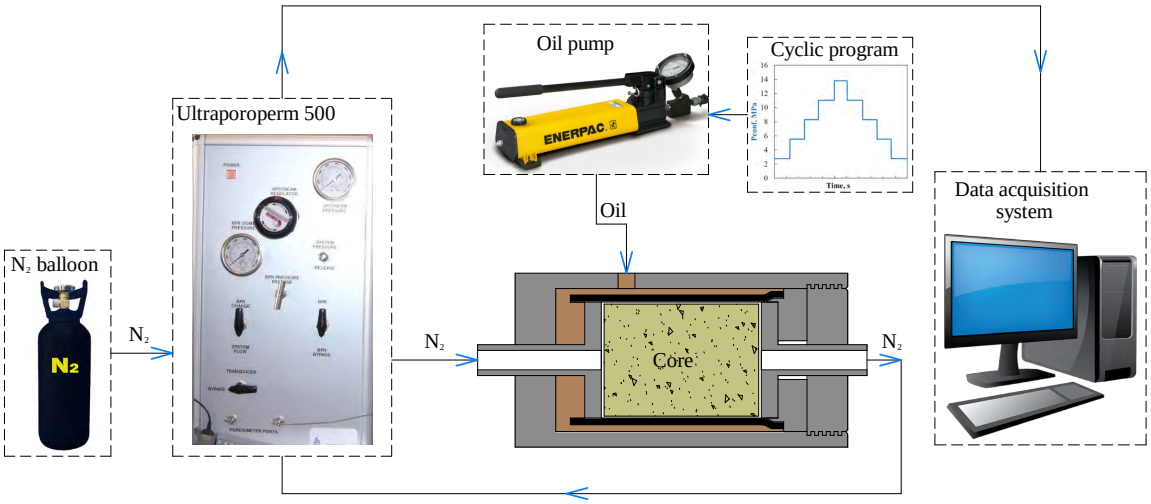

Fig. 2. Diagram of the core permeability measurement setup.

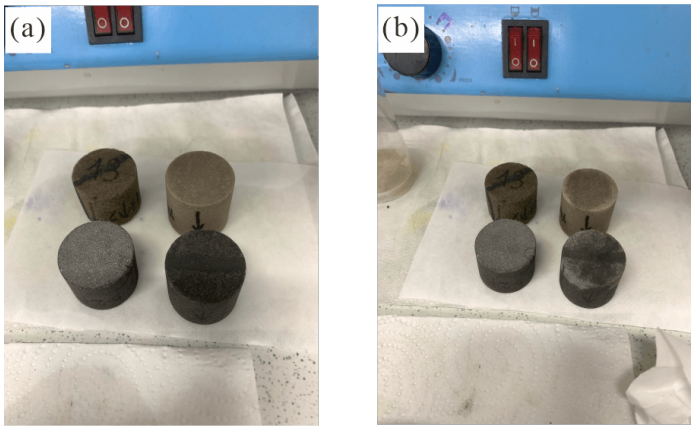

Fig. 3. (a) core samples immediately after saturation with alcohol and (b) core samples after 10 minutes of drying at room conditions.

is the atmosphere pressure (Pa), S is the samples' cross-section (m^2), P_{in} is the injection gas pressure (Pa);

5) After the first injection cycle, direct blowing is performed with a pressure gradient of 0.69 bar/cm (10 psi/cm) for 2 minutes;
6) Next, the test and blowing cycles (steps 4 and 5) are repeated several times. Depending on how permeability stabilizes, blowing was carried out in both forward and reverse directions.

Saturation/drying

7) After the primary testing, the core is removed, weighed and wrapped in filter paper, to be saturated with isopropyl alcohol. Paper is used to minimize contamination of the core during saturation. The samples were placed in a vacuum saturator so that, upon saturation, the alcohol flow coincides with the direction of the nitrogen injection during the primary testing;
8) After saturation, the filter paper is removed, and the samples are left to dry at room temperature until a constant weight is achieved (Fig. 3). The samples are positioned with the arrow on the side surface pointing downwards, indicating the direction of injection. In this position, isopropyl alcohol evaporates, and the alcohol meniscus moves from top to bottom. Thus, during evaporation, the movement of the alcohol meniscus causes colloids to migrate in the forward direction;

Secondary testing

9) After drying the samples to constant weight, research is carried out by program for Primary testing (points 2-6).

The cyclic test program is similar to the procedure described in the work (Kozhevnikov et al., 2023) where high-gradient (6.9 MPa/m) nitrogen blowings were performed between cycles in both forward and reverse directions. Fig. 4 depicts the permeability dynamics of sample No. 9 under cyclic confining pressure (Fig. 4(b)). The graphs in Figs. 4(c)-4(e) indicates that the permeability in different cycles was unpredictable and did not correspond to changes in the confining pressure. This confirms the theory that permeability changes occur due to colloidal migration. Blowings in the forward (Fig. 4(f)) and reverse (Fig. 4(g)) directions result in jumps in permeability between cycles (Figs. 4(h)-4(j)) due

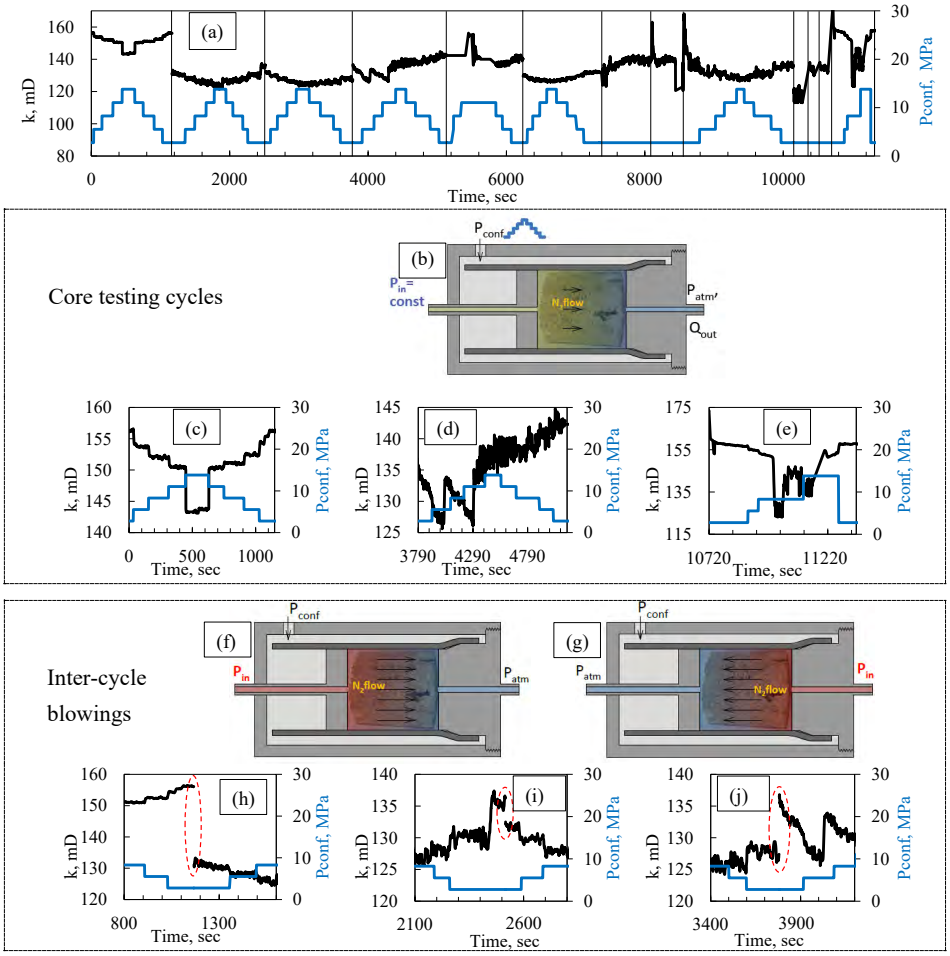

Fig. 4. (a) Permeability dynamics of sample No. 9, where the black line represents permeability and the blue line represents the confining pressure program. Vertical lines indicate blowings between cycles, (b) schematic representation of the core in the core holder during permeability measurement, (c, d, e) examples of permeability dynamics during loading/unloading cycles, (f, g) schematic representation of the core in the core holder during blowings, and (h, i, j) jumps in permeability between cycles as a result of blowings.

to colloid migration.

3. Results and discussion

Permeability dynamics over time under cyclic loading are presented in Fig. 5. A stepwise increase and decrease in confining pressure are one cycle; blowings were carried out between cycles at a minimum confining pressure of 2.76 MPa. The graphs do not show blowings and their direction; the cycles are not numbered to avoid overloading the graphs.

Analysis of the permeability dynamics under cyclic loading allowed the following general observations to be drawn.

3.1 Primary testing

In limestone samples, blowings led to unpredictable changes in permeability. For sample No. 1, permeability remains stable during primary testing, with consistent changes in each cycle (red line, Fig. 5(a)) due to elastic deformations. In sample No. 6, a significant decrease in permeability is observed during unloading in the first cycle, which is unusual for mechanical compaction. Generally, the effect of blowing on permeability is noted only at the end of primary testing (red line, Fig. 5(b)). During primary testing, samples No. 9 and 20 exhibit a substantial decrease in permeability after the first blowing between the first and second cycles (red line in Figs. 5(c) and 5(d)). In subsequent cyclic loading, permeability changes unpredictably, with observed jumps in permeability between blowings.

In sandstone samples, the effect of blowings on permeability is less clear, with minimal visible jumps in permeability between cycles on the graph (Figs. 5(e)-5(h)). Permeability dynamics primarily result from deformations and coincide with the loading path in all cycles (Figs. 5(e)-5(h)).At maximum load, the permeability of samples 51 and 61 remains constant, although the initial permeability is slightly higher than the final value, indicating incomplete opening of microcracks during unloading. For samples No. 131 and 181, an increase in permeability is observed with each subsequent cycle at maximum load, and at the end of primary testing, the permeability exceeds the initial value. In highly permeable

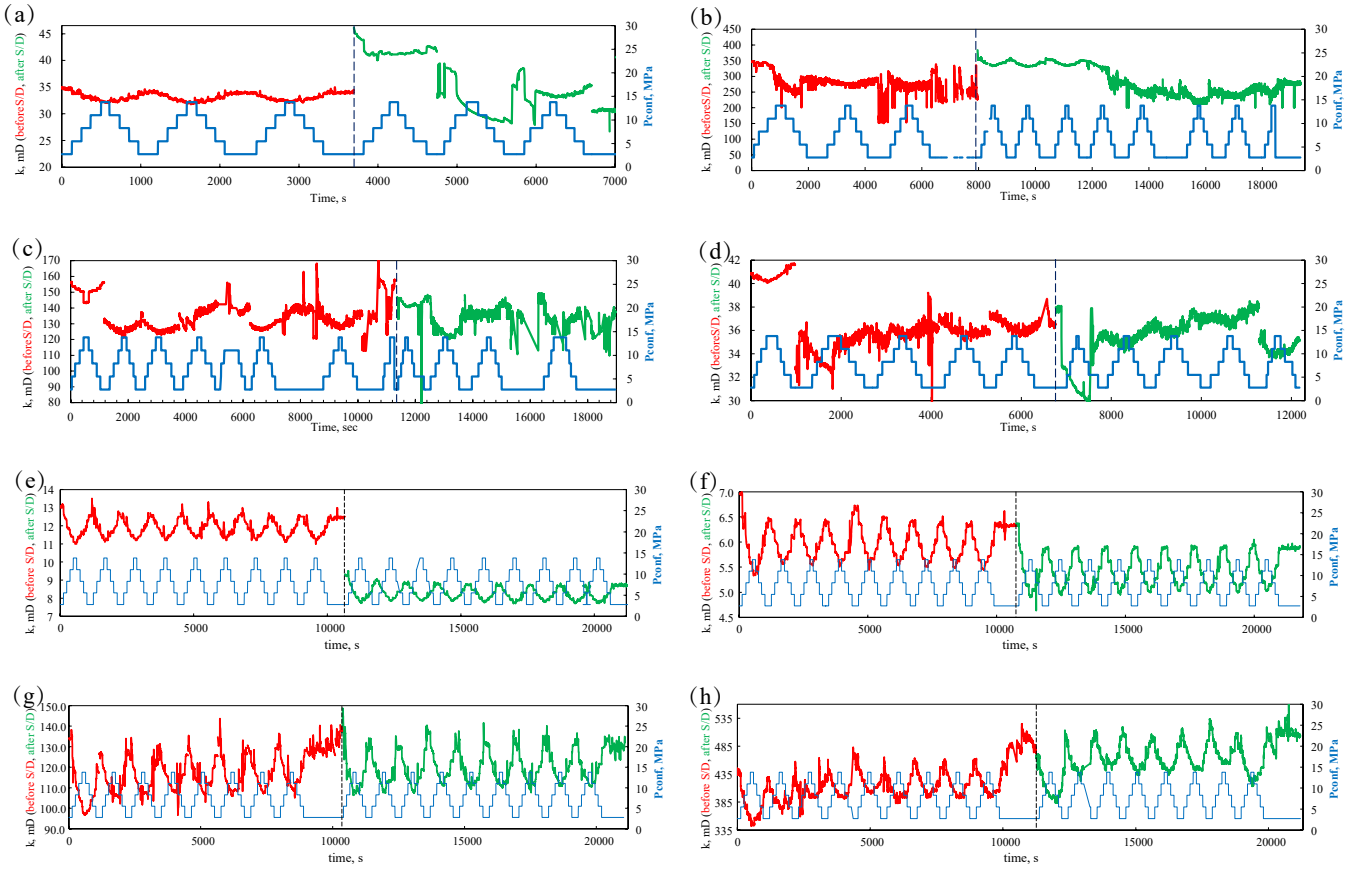

Fig. 5. Dynamics of permeability under cyclic confining pressure for core samples (a) 1, (b) 6, (c) 9, (d) 20, (e) 51, (f) 61, (g) 131 and (h) 181. The red solid line is permeability before saturation, the green line is after drying, the blue solid line is confining pressure. The vertical dotted line shows the boundary between tests at which samples were saturated and dried.

samples No. 131 and 181, residual deformations have minimal impact on permeability.

3.2 Secondary testing after saturation and drying

Primary testing indicated that blowings did not affect the permeability dynamics in all samples, possibly due to insufficient detachment force. Additionally, in specific samples, a permanent decrease in permeability occurred after initial cyclic testing for unclear reasons. To induce colloid migration or eliminate potential colloidal plugs, the internal equilibrium of the samples was disrupted by saturating them with isopropyl alcohol and drying them.

After the saturation and drying procedure, the following observations were made.

The saturation and drying procedures greatly affected the permeability of carbonate samples. In samples No. 1 and 6, there was a significant increase in permeability at the beginning of secondary testing. Compared to primary testing, the increase in permeability was approximately 32% and 40% for samples No. 1 and 6, respectively. Additionally, in sample No. 1, blowings began to affect the permeability, resulting in jumps in permeability between cycles. However, the permeability stabilized by the end and became the same as in primary testing (green line in Fig. 5(a)). In sample No. 6, after saturation and drying for the first three cycles, the permeability corresponded to elastic deformation, and the influence of direct blowing was not observed. However, reverse blowing decreased in permeability to values similar to those at the end of primary testing (green line in Fig. 5(b)).

In sample No. 9, the saturation and drying procedure led to a slight decrease in permeability during secondary testing, causing even greater chaos in its dynamics (green line in Fig. 5(c)). In sample No. 20, after saturation and drying, the permeability became slightly higher than at the end of primary testing, but then followed a similar trend (green line in Fig. 5(d)). In both samples No. 9 and 20, the permeability during secondary testing did not correspond to the loading observed in primary testing. This suggests that other factors significantly influence the permeability.

In low-permeability sandstone samples No. 51 and 61, there is an overall decrease in permeability after saturation and drying compared to the primary testing (Figs. 5(e) and 5(f)). The saturation and drying procedure did not significantly alter the permeability path, which remained unchanged throughout loading cycles after blowing. The absolute value of permeability amplitude during loading and unloading decreased from approximately 1.8 mD in primary testing to about 1.4 mD in

secondary testing. Still, the percentage ratio remained constant at around 15%.

In samples No. 131 and 181, no noticeable changes were observed after saturation and drying. Both samples exhibited a gradual increase in permeability during cyclic loading, which contradicts the theory of mechanical compaction's influence on permeability.

According to the classical theory, the main reason for changes in permeability under loading is the mechanical compaction of rocks due to elastic and plastic deformations, as observed in our laboratory studies. However, the permeability dynamics under loading also exhibit the following features:

- Residual deformations and creep do not cause jumps in permeability between blowings, as the confining pressure is low and constant, and blowing lasts a relatively short time (2 minutes).
- The permeability dynamics in each cycle differ and sometimes do not correspond to the confining pressure, especially in limestone samples.
- Saturation and drying result in different changes in permeability for samples, despite using rock-neutral liquid (isopropyl alcohol). Some samples show noticeable increases in permeability, while others experience decreases.
- In some samples, permeability increases during cyclic loading, both during primary testing and after saturation and drying. This increase cannot be attributed to dilatation due to the relatively low confining pressure. The maximum confining pressure is 13.8 MPa, three times lower than natural rock pressure, making plastic deformations unlikely.

The listed facts indicate that extraneous factors influence the permeability of samples in addition to deformations. Colloid migration plays a role in changing the transport properties of rocks, as indicated by studies (Kozhevnikov et al., 2021, 2022a, 2023; Turbakov et al., 2022; Riabokon et al., 2023). The mechanism of colloid migration's influence on permeability is described in Fig. 6. During primary testing, colloids detach from pore walls and accumulate in bottlenecks, reducing the transport properties of the porous medium (Fig. 6(a)). In the first cycle, colloid migration occurs extensively, but its effect on permeability under loading remains uncertain. During unloading, colloids should affect permeability, resulting in anomalous dynamics: increased permeability due to pore unblocking or a continuing decrease. Examples of anomalous permeability dynamics in the first cycle are shown in Figs. 5(b) and 5(d) for samples No. 6 and 20, respectively. In other samples, the exact cause of the permeability decrease is unclear, and classic permeability hysteresis, typically attributed to mechanical compaction, is observed. The influence of colloids on permeability dynamics is not observable for two reasons. Firstly, colloids may be absent, and secondly, the nitrogen flow is insufficient for colloid migration. In cases where colloids are initially absent in the samples, the first cyclic loading can result in micro-fractures, grain disintegration, and cement fragmentation. Blowings were conducted between cycles to assess the presence and migration of colloidal particles and their impact on permeability. Blowings facilitate enhanced particle detachment, migration, and pore blockage (Fig. 6(b)). Forward blowing leads to a decrease in permeability (Fig. 6(b)), while reverse blowing causes an increase in permeability. After blowing, the particles become poorly mobile in a porous medium due to increased Coulomb forces when electrostatically charged by a flow. They occupy stable positions in narrow areas, blocking pores (Fig. 6(c)) and reducing permeability. This effect is evident in the jumps observed in the permeability dynamics of samples No. 9 and 20 during primary testing, and sample No. 1 during secondary testing. In subsequent cycles, the flow velocity is low and insufficient to detach and move particles, resulting in stable permeability dynamics (Deb and Chakma, 2022; Kozhevnikov et al., 2022b). This phenomenon is observed in the second cycle across all samples. The effect of blowing on permeability is not observable in other limestone samples and all sandstones.

More force must be applied to detach particles, which can be achieved by a higher flow rate or a change in the viscosity of the injected agent. In our work, to mobilize stuck colloids after primary testing, we saturated samples with isopropyl alcohol and then dried them at room conditions without load. Saturation with fluid facilitates the mobilization of particles due to surface tension, similar to the observed 'coffee ring' effect (Mampallil and Eral, 2018). The 'coffee ring' effect refers to the movement of colloidal particles within a droplet during evaporation. When core samples are saturated, fluid moving along the pore channel detaches colloids from the walls through surface tension (Fig. 6(d)). Dispersed colloids within the fluid can migrate through the pores and accumulate in the pore throats (Fig. 6(e)). During evaporation, the moving alcohol meniscus, with high colloid concentrations, blocks pore throats (Fig. 6(f)). Since the flow of alcohol does not have a clear direction from one face of the sample to another due to the heterogeneity of the porous medium and wetting from the side surface upon saturation, colloidal movement can occur in any direction, potentially blocking pores either along the injection path of nitrogen (Fig. 6(g)) or in the reverse direction (Fig. 6(i)). In either case, the movement of colloidal particles during saturation and drying can be indirectly determined by the dynamics of permeability in secondary testing, as observed in the results of our studies (Fig. 5).

In addition to colloid migration, saturation with isopropyl alcohol leads to the detachment of new particles. Under cyclic loading, sufficiently large particles inside a porous medium can crack but remain attached to the matrix (Fig. 1(d), Fig. 6, large dark blue particle). Since these particles remain attached to the matrix, detachment during gas injection is impossible due to insufficient force. Upon saturation, microcracks become wetted and experience growth due to the Rehbinder's wedging effect, resulting in detachment and liberation of large particles (Figs. 6(d)-6(f)). However, the mobility of these particles is limited due to their size, preventing them from moving far with the flow (Figs. 6(g)-6(i)). Large particles can only roll within a few pores, significantly affecting pore conductivity. As a result, subsequent blowing cannot displace them, leaving permeability unaffected. This effect is observed

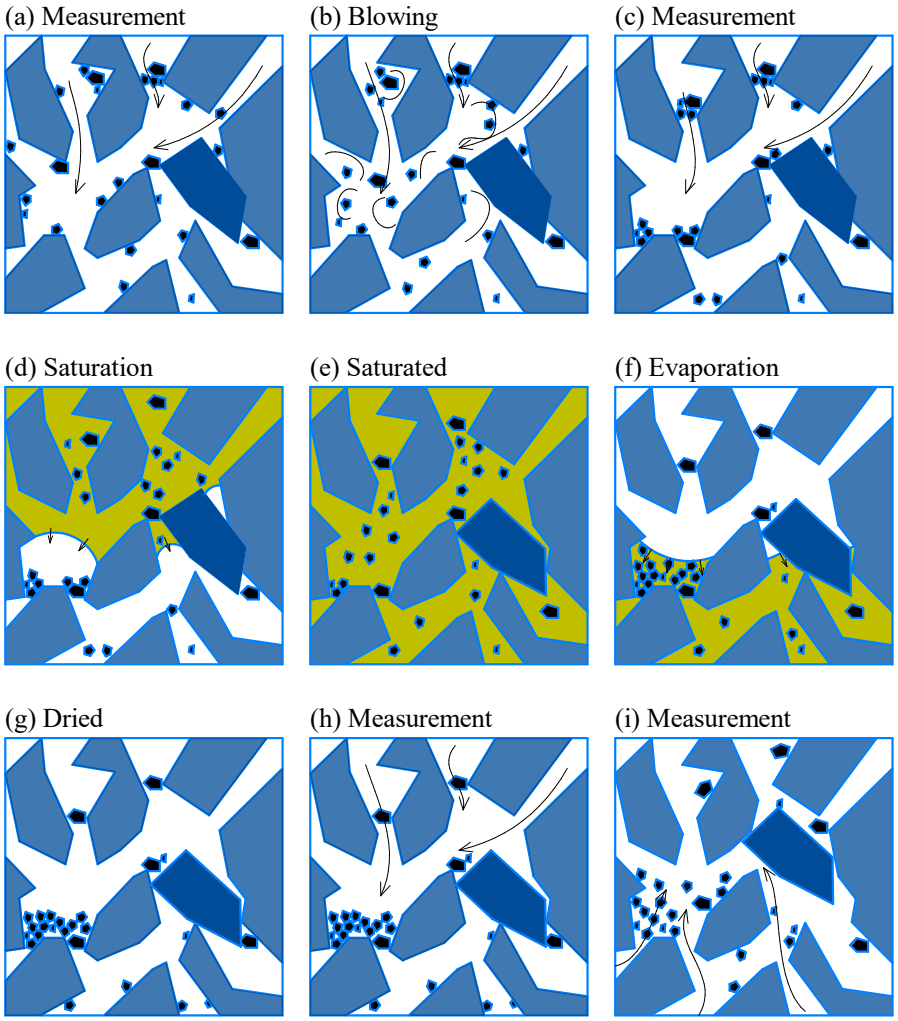

Fig. 6. Schematic representation of colloid migration during the first core test (a-c). (a) migration of colloids during permeability measurements, (b) migration of colloids during blowings, (c) state of the porous medium after blowings, (d) Migration of colloids during saturation, (e) Dispersed colloids and detached particles in saturated porous media, (f) Migration of colloids during drying, (g) The distribution of colloids and detached particles in a porous medium after saturation/drying, (h) during permeability measurements in the forward, and (i) reverse directions. The rock matrix is represented by light blue, while colloids and weakly attached particles are depicted in dark blue. Black arrows indicate the direction of nitrogen flow in tests, and yellow indicates isopropyl alcohol used for saturation.

in low-permeability sandstone samples No. 51 and 61. In secondary testing, the permeability became significantly lower (Figs. 5(e) and 5(f)), but the dynamics under cyclic loading remained unchanged. Evidence of particle detachment due to wetting is observed through changes in sample mass and the presence of sand grains in the filter paper after saturation. In limestones, the decrease in mass before and after saturation is approximately 0.002 g, which is close to the measurement error. Limestones are more consolidated and fine-grained. In limestones, the destruction of grains on surfaces due to compression is not observed. A change in permeability at a constant mass after saturation and drying indicates internal migration of particles and minimal destruction of surface grains in limestones. In sandstones, the decrease in mass is more noticeable after saturation and drying, ranging from 0.02 to 0.042 g. The most significant decrease in mass occurs in the more porous and coarse-grained samples No. 131 and 181. In granular sandstones, mechanical cracking of some grains occurs without separation under dry conditions when loaded. The same damage occurs inside the samples, leading to particle detachment and a change in permeability. The greatest effect from destruction upon saturation is observed in samples where the size of the particles being broken off is comparable to the size of the pore throats. This explains the significant decrease in permeability observed in sandstone samples No. 51 and 61, while in samples 131 and 181, permeability remains the same at the beginning of secondary testing.

After drying, an initial state is formed inside the pore space due to the transfer of colloids and the detachment of new free particles due to alcohol saturation (Fig. 6(g)). The movement of alcohol during saturation and drying may not only be axial in the forward but also radial and reverse directions due to

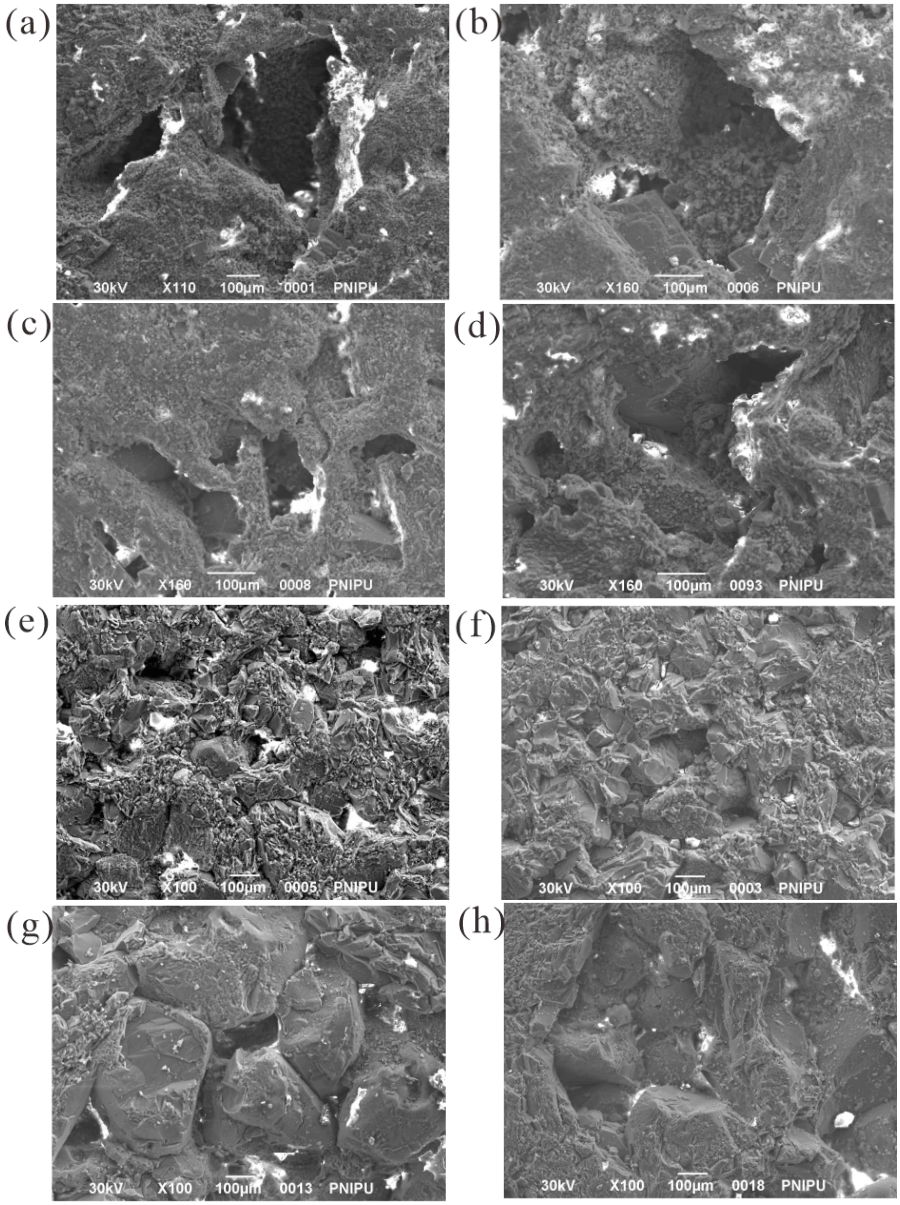

Fig. 7. Microphotographs of samples No. (a) 1, (b) 6, (c) 8, (d) 9, (e) 51, (f) 61, (g) 131 and (h) 181. All photographs are given with the same scale to compare the sizes of pores and grains.

the sample's heterogeneity. Consequently, when measuring permeability, colloidal plugs can be directed (Fig. 6(h)) or reversed (Fig. 6(i)) relative to the flow and the permeability may increase (Figs. 5(a), 5(b), 5(d) and 5(g)) or decrease (Figs. 5(c), 5(e), 5(f) and 5(h)).

Different samples exhibit varying permeability dynamics. The impact of blowings, saturation, and drying procedures is more pronounced in limestone samples, while sandstones show less susceptibility to changes in permeability. The study conditions foster the mobilization and migration of colloids within a porous medium, leading to the blocking and unblocking of pore channels. The injection involved the same flow rate, ensuring equal detachment forces for all samples. However, the structure, shape of grains, and pore space geometry differ across the samples, influencing the number and size of colloids present, and potential colloid traps, such as bottlenecks. Micrographs in Fig. 7 display sample surfaces, all presented on the same scale to easily compare pore structure and size. Microstructure analysis reveals that limestone samples possess a fine-crystalline structure with secondary crystals on pore walls (Figs. 7(a)-7(d)). These seemingly well-attached small crystals could be a primary source of colloids within the pores, as their deformation during loading contributes to detachment. Another factor contributing to pore blockage is the ability of particles to migrate within the pores, affecting their accumulation in bottlenecks. Larger pores in a medium not only facilitate the formation of larger debris but also enable more profound particle migration, resulting in a more significant decrease in permeability. These assumptions are validated through experimental evidence. In limestone

samples, the irregular shape of the pores (Figs. 7(a)-7(d)) contributes to the breakage of large crystals that can obstruct highly conductive pores. This observation is reflected in the permeability dynamics observed after blowings (Figs. 5(a)-5(d)).

In sandstones, the impact of blowing is not visible. The slightest influence of blowing was observed in samples with low permeability (No. 51 and 61). Samples No. 131 and 181 exhibit permeability dynamics that do not correspond to mechanical compaction, possibly due to colloid migration. The lack of blowing influence on samples No. 51 and 61 can be explained by their dense matrix and relatively large quartz grains, comparable to or larger than pore size (Figs. 7(e)-7(f)). Moreover, detachment of new crystals is unlikely under low loads and dry conditions. Even if they exist, these crystals cannot move deeper and remain confined within the pore. Since samples No. 51 and 61 have pore sizes similar to crystals, particle cracking leads to a decrease in permeability. In highly porous sandstones, individual channel blockage has insignificant effects on overall permeability change. The main source of colloids in highly permeable sandstone samples No. 131 and 181 is cement, which has lower strength and tends to chip when located on the edges of quartz grains. The limited presence of cement in the sandstone samples explains the minimal impact of blowing and the saturation and drying procedure on permeability dynamics.

4. Conclusions

The paper presents the results of laboratory studies on the influence of cyclic loading on the transport properties of limestone and sandstone samples. The research results confirm our earlier theory that the migration of colloids affects its dynamics when measuring permeability. An additional mechanism for assessing the effect of colloid migration on permeability is proposed. It involves saturating and drying core samples with isopropyl alcohol between cyclic tests. The following conclusions were obtained:

1) The observed permeability dynamics indicate a significant influence of colloid migration during measurements. In limestone samples, the effect of colloidal migration is visible, manifesting as jumps in the permeability line between cycles. This discrepancy between permeability and the loading path is not a result of residual deformations and creep. The effect of colloid migration on the permeability dynamics of sandstone samples is less obvious.
2) The permeability dynamics on each cycle differ and sometimes do not correspond to the confining pressure.
3) The new technique allows for the verification of colloid migration and shows that the initial permeability of the samples can deteriorate.
4) Saturation and drying of samples lead to different changes in permeability. Saturation and subsequent drying promote the migration of colloids within the pore space. When wetting, isopropyl alcohol removes the electrostatic charge from colloidal particles, detaching them into the fluid volume. During drying, the meniscus movement promotes the movement of colloidal particles more profoundly into the pore space due to surface tension, similar to the "coffee ring effect". The proposed concept correlates well with the change in permeability at the end of the primary and at the beginning of the secondary testing during saturation and drying, further confirming the theory about the influence of colloids when measuring permeability.
5) The change in mass and permeability after saturation and drying shows that the slight change in mass of limestone means that few particles break off from the surface of the samples. However, the permeability changes significantly, indicating particle movement within the pore space. In sandstones, the change in mass is significant due to the spalling of particles by the Rehbinder effect.

The research results can be used to model natural gas or hydrogen reservoir permeability during filling and emptying cycles. During injection, the rocks around the well dry, and during gas withdrawal, water enters and wets the porous medium. It is essential to consider the migration of colloids during saturation and drying when injecting and withdrawing gases.

Acknowledgements

This research was funded by the Russian Science Foundation project (No. 23-19-00699), https://rscf.ru/project/23-19-00699/.

Additional information: Author's email

rinapan01@mail.ru (A. Panteleeva);
zakhar.ivanov.2013@gmail.com (Z. Ivanov).

Conflict of interest

The authors declare no competing interest.

References

Almutairi, A., Saira, S., Wang, Y., et al. Effect of fines migration on oil recovery from carbonate rocks. Advances in Geo-Energy Research, 2023, 8(1): 61-70.

Anyim, K., Gan, Q. Fault zone exploitation in geothermal reservoirs: Production optimization, permeability evolution and induced seismicity. Advances in Geo-Energy Research, 2020, 4(1): 1-12.

Bedrikovetsky, P., Siqueira, F. D., Furtado, C. A., et al. Modified particle detachment model for colloidal transport in porous media. Transport in Porous Media, 2011, 86: 353-383.

Blöcher, G., Kluge, C., Milsch, H., et al. Permeability of matrix-fracture systems under mechanical loading-constraints from laboratory experiments and 3-D numerical modelling. Advances in Geosciences, 2019, 49: 95-104.

Chen, L., Zhang, D., Zhang, W., et al. Experimental investigation on post-Peak permeability evolution law of saturated sandstone under various cyclic loading-unloading and confining pressure. Water, 2022, 14(11): 1773.

Civan, F. Effective-Stress coefficients of porous rocks involving shocks and loading/unloading hysteresis. SPE Journal, 2021, 26(1): 44-67.

Deb, D., Chakma, S. Colloid and colloid-facilitated contaminant transport in subsurface ecosystem-a concise review. International Journal of Environmental Science and Technology, 2022, 20: 6955-6988.

Gao, Y., Chen, M., Pang, H. Experimental investigations on elastoplastic deformation and permeability evolution of terrestrial Karamay oil sands at high temperatures and pressures. Journal of Petroleum Science and Engineering, 2020, 190: 107124.

Ge, J., Saira, Smith, B., et al. Laboratory comparison of tertiary N_2, CH_4, and CO_2 injection into an Inland oil field sample. Fuel, 2022, 324: 124635.

Haghi, A. H., Chalaturnyk, R., Geiger, S. New semi-analytical insights into stress-dependent spontaneous imbibition and oil recovery in naturally fractured carbonate reservoirs. Water Resources Research, 2018, 54: 9605-9622.

Heller, R., Vermylen, J., Zoback, M. Experimental investigation of matrix permeability of gas shales. AAPG Bulletin, 2014, 98: 975-995.

Hofmann, H., Blöcher, G., Milsch, H., et al. Transmissivity of aligned and displaced tensile fractures in granitic rocks during cyclic loading. International Journal of Rock Mechanics and Mining Sciences, 2016, 87: 69-84.

Hu, C., Agostini, F., Jia, Y. Porosity and permeability evolution with deviatoric stress of reservoir sandstone: Insights from triaxial compression tests and in situ compression CT. Geofluids, 2020, 2020: 6611079.

Kluge, C., Blöcher, G., Hofmann, H., et al. The stress-memory effect of fracture stiffness during cyclic loading in low-permeability sandstone. Journal of Geophysical Research: Solid Earth, 2021, 126: e2020JB021469.

Kozhevnikov, E., Riabokon, E., Turbakov, M. A model of reservoir permeability evolution during oil production. Energies, 2021, 14(9): 2695.

Kozhevnikov, E. V., Turbakov, M. S., Gladkikh, E. A., et al. Colloidal-induced permeability degradation assessment of porous media. Géotechnique Letters, 2022a, 12: 217-224.

Kozhevnikov, E. V., Turbakov, M. S., Gladkikh, E. A., et al. Colloid migration as a reason for porous sandstone permeability degradation during coreflooding. Energies, 2022b, 15(8): 2845.

Kozhevnikov, E. V., Turbakov, M. S., Riabokon, E. P., et al. Effect of effective pressure on the permeability of rocks based on well testing results. Energies, 2021, 14(8): 2306.

Kozhevnikov, E. V., Turbakov, M. S., Riabokon, E. P., et al. Apparent permeability evolution due to colloid migration under cyclic confining pressure: On the example of porous limestone. Transport in Porous Media, 2023, in press, https://doi.org/10.1007/s11242-023-01979-5.

Lei, G., Liao, Q., Lin, Q., et al. Stress dependent gas-water relative permeability in gas hydrates: A theoretical model. Advances in Geo-Energy Research, 2020, 4(3): 326-338.

Li, M., Xiao, W. L., Bernabé, Y., et al. Nonlinear effective pressure law for permeability. Journal of Geophysical Research: Solid Earth, 2014, 119: 302-318.

Liu, C., Yu, B., Zhang, D., et al. Experimental study on strain behavior and permeability evolution of sandstone under constant amplitude cyclic loading-unloading. Energy Science & Engineering, 2020, 8: 452-465.

Liu, W., Li, Y., Wang, B. Gas permeability of fractured sandstone/coal samples under variable confining pressure. Transport in Porous Media, 2010, 83: 333-347.

Mampallil, D., Eral, H. B. A review on suppression and utilization of the coffee-ring effect. Advances in Colloid and Interface Science, 2018, 252: 38-54.

Metwally, Y. M., Sondergeld, C. H. Measuring low permeabilities of gas sands and shale using a pressure transmission technique. International Journal of Rock Mechanics and Mining Sciences, 2011, 48: 1135-1144.

Milsch, H., Hofmann, H., Blöcher, G. An experimental and numerical evaluation of continuous fracture permeability measurements during effective pressure cycles. International Journal of Rock Mechanics and Mining Sciences, 2016, 89: 109-115.

Nolte, S., Fink, R., Krooss, B. M., et al. Simultaneous determination of the effective stress coefficients for permeability and volumetric strain on a tight sandstone. Journal of Natural Gas Science and Engineering, 2021, 95: 104186.

Raziperchikolaee, S. Impact of stress dependence of elastic moduli and poroelastic constants on earth surface uplift due to injection. Advances in Geo-Energy Research, 2023, 10(1): 56-64.

Riabokon, E., Gladkikh, E., Turbakov, M., et al. Effects of ultrasonic oscillations on permeability of rocks during the paraffinic oil flow. Géotechnique Letters, 2023, 13(3): 151-157.

Selvadurai, A. P. S., Głowacki, A. Permeability hysterisis of limestone during isotropic compression. Groundwater, 2008, 46: 113-119.

Siqueira, F. D., Yang, Y., Vaz, A., et al. Prediction of productivity decline in oil and gas wells due to fines migration: Laboratory and mathematical modelling. Paper SPE 171475 Presented at the SPE Asia Pacific Oil & Gas Conference and Exhibition, Adelaide, Australia, 14-16 October, 2014.

Stanton-Yonge, A., Mitchell, T. M., Meredith, P. G. The hydro-mechanical properties of fracture intersections: pressure-dependant permeability and effective stress law. Journal of Geophysical Research: Solid Earth, 2023, 128: e2022JB025516.

Torkzaban, S., Bradford, S. A., Vanderzalm, J. L., et al. Colloid release and clogging in porous media: Effects of solution ionic strength and flow velocity. Journal of Contaminant Hydrology, 2015, 181: 161-171.

Turbakov, M. S., Kozhevnikov, E. V., Riabokon, E. P., et al. Permeability evolution of porous sandstone in the initial period of oil production: Comparison of well test and coreflooding data. Energies, 2022, 15(17): 6137.

Vogler, D., Amann, F., Bayer, P., et al. Permeability evolution in natural fractures subject to cyclic loading and gouge formation. Rock Mechanics and Rock Engineering, 2016, 49: 3463-3479.

Wang, D., Qian, Q., Zhong, A., et al. Numerical modeling of micro-particle migration in channels. Advances in Geo-Energy Research, 2023, 10(2): 117-132.

Wang, W., Duan, X., Jia, Y., et al. Deformation characteristics, gas permeability and energy evolution of low-permeability sandstone under cyclic loading and unloading path. Bulletin of Engineering Geology and the Environment, 2022, 81: 369.

Wu, Q., Tang, T., Zhao, Z., et al. Influence of micro-particles on gas hydrate formation kinetics: Potential application to methane storage and transportation. Advances in Geo-Energy Research, 2023, 10(3): 189-199.

Xin, T., Liang, B., Wang, J., et al. Experimental study on the evolution trend of the pore structure and the permeability of coal under cyclic loading and unloading. ACS Omega, 2021, 6(51): 35830-35843.

Yang, S., Hu, B. Creep and long-term permeability of a red sandstone subjected to cyclic loading after thermal treatments. Rock Mechanics and Rock Engineering, 2018, 51(1): 2981-3004.

Yang, S., Xu, P., Ranjith, P. G., et al. Evaluation of creep mechanical behavior of deep-buried marble under triaxial cyclic loading. Arabian Journal of Geosciences, 2015, 8(9): 6567-6582.

Zheng, J., Zheng, L., Liu, H. H., et al. Relationships between permeability, porosity and effective stress for low-permeability sedimentary rock. International Journal of Rock Mechanics and Mining Sciences, 2015, 78: 304-318.

Zhou, Z., Zhang, J., Cai, X., et al. Permeability evolution of fractured rock subjected to cyclic axial load conditions. Geofluids, 2020, 2020: 4342514.